Frontiers in Scientific Research and Technology

Online ISSN: 2682-2970
Print ISSN: 2682-2962
http://fsrt.journals.ekb.eg

FSRT J 6 (2023) 29 - 40 10.21608/FSRT.2023.199760.1088

Optical chemo sensors based on nanocellulose for selective detection of hazardous pollutants: A review

Rasha M. Kamel[a], Ahmed Shahat[a], Manar M. Abd El-Emam[a], Esraa M. Kilany[b,*]

[a] *Suez University, Faculty of Science, Chemistry Department, 43518 Suez, Egypt*
[b] *Suez University, Faculty of Petroleum and Mining Engineering, Science and Mathematics Department, Suez, Egypt*

ARTICLE INFO

Article history:
Received 27 March 2023
Received in revised form 12 April 2023
Accepted 13 April 2023
Available online 18 April 2023

Keywords
Nanocellulose,
Cellulose microfibrils
Cellulose nanocrystals
Detection

ABSTRACT

Cellulose is a significant widespread sustainable resource on earth. With the development of nanotechnology, the interest of cellulose scientists has moved to the separation of nanocellulose from many plants and their application in technical applications. The promising properties of nanocellulose and related products are driving rapid progress in nanocellulose chemistry and engineering. In fact, nanocelluloses integrate cellulose's essential features with the exceptional properties of nanoscale materials. This paper summarizes modern knowledge in nanocellulose research and development. The methods for synthesizing nanocellulose and its functionalization procedures will be discussed after an introduction to the chemical structure and microfibrillar organization of nanocellulose in cellulose bundles with other components. Finally, the usage of nanocellulose for pollutant detection will be discussed.

1. Introduction

Nanotechnology is stated as the modification and implementation of substances with dimensions of 100 nm or lower in at least a single dimension, and whose physical, chemical, or biological characteristics differ significantly from those of the bulk substance [3].

In recent times, nanotechnology has attracted the interest of numerous industries, opening up countless innovative prospects, especially in the wood manufacturing and cellulose-based materials. The study and development of material with one dimension at least ranging from 1 to 100 nm is referred to as nanotechnology. Chemical or mechanical procedures on the pulp of cellulose can produce nanometeric cellulose, like cellulose nanofibrils (CNFs) and cellulose nanocrystals (CNCs). As compared to the bulk material as well as other substances like Kevlar, carbon fibers, and stainless steel, nanocellulose has achieved exceptional qualities. [1, 2].

Although nanocellulose has not yet become an economically viable material, *CelluForce* in Canada launched the first factory for CNC manufacture and disposal in 2012, producing approximately one tone of crystalline nanocellulose each 24 hours.

There are additionally certain nanocellulose research sites around the world, with *Innventia* starting one of the first in Sweden around 2011, opened initial production site inside the United States in Madison within 2012 as it is the state's biggest manufacturer of noncellulosic products, providing both crystalline nanocellulose and nanofibrils from TEMPO treatment. The production plant's goal is to help with the production and marketing of nanocellulose materials by supplying working quantities to investigators and customers in the sector.

Increasing understanding of nanocellulose and creating strategies for controlling its characteristics through manufacturing can provide novel possibilities for the development of products. Superior biobased products can be developed and used to replace products that based on fossil fuel. There have been some studies published about nanocellulose, the majority of which focus on nanocellulose as a carrier substance in bio-composites and the usage of nanocellulose from bacteria (BNC) in medicinal or clinical applications. [1, 3, 4].

Nanocellulose, also known as nanocrystals, whiskers, rods, and nanofibrils is a cellulosic fibre crystalline cellulose that has at least one dimension in the nanometeric scale. *TAPPI* released a strategy to set up international nanocellulose standards. in 2011, stating that the acronyms for significant nanocelluloses are: cellulose nanocrystals (CNCs), cellulose nanofibrils (CNFs), and cellulose microfibrils (CMFs). As non-crystalline parts of cellulose nanocrystals are hydrolyzed, and the other crystalline parts are in the nanometeric scale in all regions (Fig. 1). Some of the inter-fibrillated hydrogen bonds in cellulose nanofibrils

* Corresponding author at Suez University
E-mail addresses: esraa.kilany@pme.suezuni.edu.eg
(Esraa M. Kilany)

(CNFs), further known as cellulose microfibrils (CMFs), would degrade and create fibers with micrometric long (non-crystal areas remain) and nanometeric in diameter. Bacterial nanocellulose (BNCs) is manufactured by bacteria cultivated in a culture media as microfibrils. BNC microfibrils could be hydrolyzed to bacterium nanocrystals with an acidic hydrolysis method such as crystalline nanocellulose.

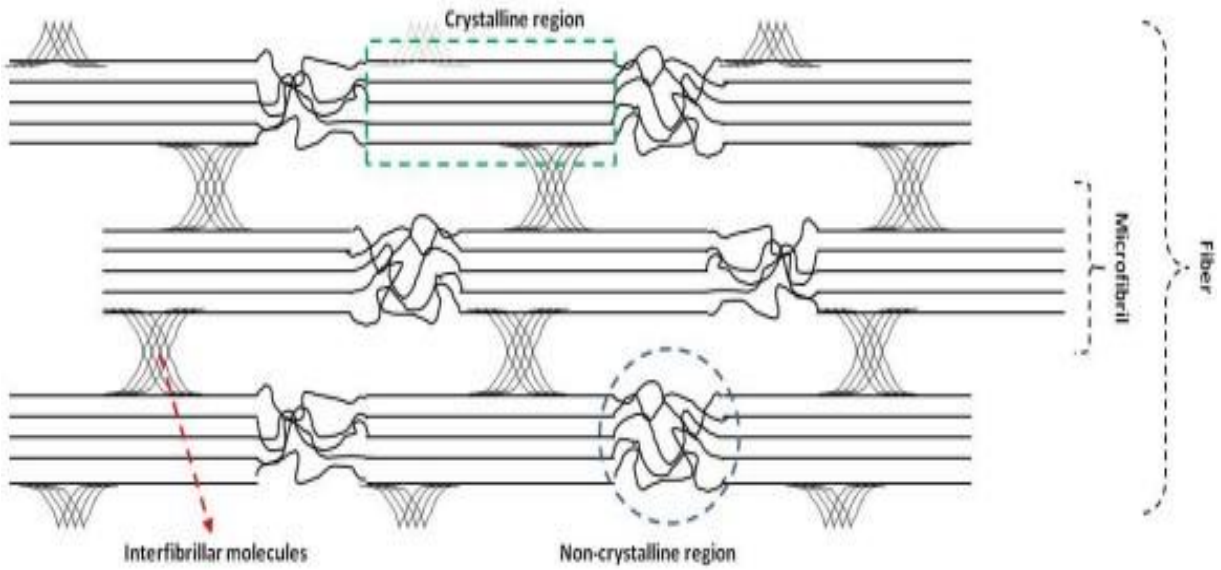

Fig. 1: section of a cellulose fiber illustrating the crystalline and non-crystalline parts [5]

Acid hydrolysis eliminates the non-crystalline areas, leaving just the crystalline areas (crystalline nanocellulose). Mechanical treatment of the fibres can maintain each of the non-crystalline and crystalline parts, while certain interfibrillar linkages would be destroyed, resulting in nanometer diameter and micrometer long fibrils (cellulose nanofibril).

2. Sources of nanocellulose

2.1 Natural fibers

The expression "natural fibre" refers to a wide variety of fibres which formed by nature through plants, animals, and minerals **[6]**. In order minimizing ambiguity, it is essential to mention that the attention here focuses on natural plant-based fibres and lignocellulosic fibres. As well as, non-plant cellulosic origins, like bacteria or marine creatures, are briefly discussed as well. The biodegradability of natural fibres, combined with their cheap cost, superior particular force, and lower weight than glass, has resulted in substantial development of this ecofriendly green material [7].

Natural fibers are mainly composed of cellulose, lignin, and hemicellulose. Pectin, proteins, and extractives were presented in small amounts. Cotton, bacteria, and algae, on the other hand, could become lignin and/or hemicellulose-free. Algal cellulose is refused because it has a lower cellulose percentage and couldn't become a commercial supply of nanocellulose. Natural fibers have a complex chemical constituents and cell arrangement. Each fibre is basically a compound composed of tough cellulose microfibrils inserted in a soft medium primarily consisting of lignin and hemicellulose.

2.1.1 Cellulose nanofibers/micro-fibrillated cellulose (CNF)

The lignocellulosic fibre cell wall contains fundamental thematic elements termed as elementary fibrils. The width of the elementary fibrils is ranging of 2-20 nm and they are few micrometer long. Since nanofiber size is defined as 100 nm in one dimension, these cellulose microfibrils could be considered cellulose nanofibrils. These CNFs are composed up of sets of cellulose chains that are held to each other by hydrogen bonds. The cellulose compounds are always generated as nanofibrils; up to 100 glucan chains combine to create cellulose nanofibers [8]. Grinding, refining, cryocrushing, high pressure homogenization, and other mechanical methods could be used in isolation of CNF. A standard mechanical process for CNF is refining of the pulp then homogenization that individualizes the nanofibrils and produces a good suspension when added in water. The regenerating and electrospinning of cellulose polymeric matrix is another way for manufacturing CNF. [3]. CNF was prepared utilizing chemo-mechanical processes from flax fibers, Kraft pulp, and hemp fibers before being applied as a reinforcement material in a polyvinyl alcohol (PVA) mixture.

2.1.1.1 Mechanical processing of cellulose fibres

The mechanical processing for pulp fibres begins with pulp refining and is continued by homogenization under high pressure to produce individual cellulose nanofibrils. To clarify cellulose fibres and reduce levels of lignin, hemicellulose, and pectin, chemical methods are sometimes required prior to mechanical treatment. It's primarily a couple of methods for extracting fibers prior to homogenizing of the nanofibril matrix: applying a refiner or cryocrushing. A diluted cellulose mixture (1-2 weight. %) will applied to strains inside a refiner or blender fitted with

bars, where fibres will placed under successive cyclic pressures that modify size and morphology of the fibres [3, 9].

Another technique to obtain cellulose fibres is cryocrushing. A liquid nitrogen-frozen matrix is crushed by mechanical way results in the release of cellular wall fragments produced by ice crystals produced within the pulp cell wall [10]. After dilution in water, the fine particles are homogenised in a homogenizer to produce a CNF mixture. Chemical treatment of cellulose fibres can be utilized as a pre-treatment prior to refinement to facilitate mechanical treatment of fibres and decrease energy consumption. Pretreatment can be enzymatic or involving charged groups to the fibre surface, such as carboxylation and TEMPO-oxidation (A wide range of oxidation reactants can oxidize cellulose. Cellulosic hydroxyls are capable of being transformed into aldehyde, ketone, or carboxyl groups. TEMPO is a stable and water-soluble nitroxyl radical that has been employed in chemical synthesis in aqueous circumstances as an excellent catalyst for selective oxidation of primary alcohol groups to aldehydes and carboxylic groups. When compared with nanocellulose generated from wood celluloses using standard high-pressure homogenization without chemical pretreatment, TEMPO-oxidized cellulose nanofibers exhibit several distinct features. The pre-treatment would modify structure for these fibres, making it simpler to extract the fibre during the refinement process and therefore lowering the usage of energy.

2.1.2 Cellulose Nanocrystals (CNC)

Several terminology are being utilized in the research that describe these rod-like nanomaterials. These particles are typically known as cellulose nanocrystals. CNCs are the crystalline parts of CNFs also referred to as the monocrystalline area in cellulose [11]. Cellulose nanocrystals (CNCs) typically with diameter of 2-30 nm and hundreds of nanometers long. They were generated through the hydrolysis process of cellulose fibres, as the more accessible, disordered regions are selectively degraded. Because the non-crystalline areas function as structural flaws in the microfibrils, acidic hydrolysis produces cross fragmentation of the microfibrils into shorter nanocrystals [12].

Early in the hydrolysis process, the acid disperses into the non-crystalline regions in cellulose fibre and hydrolysis occur for glycosidic bonds. Following that, hydrolysis proceeds at easier accessible glycosidic linkages within matrix, and lastly at the reducing end group and surface of the nanocrystals. The acid work much difficult to hydrolyze the glycosidic linkages as reaction proceeded.

Many different cellulose sources have been hydrolyzed to produce cellulose nanocrystals, including hardwood pulp, banana fibers, microcrystalline cellulose, cotton, , bacterial cellulose, algal fibers, sugar beet, and tunici. Chitin, potato pulp, yellowish peas, and waxy maize are other polymers that found to generate nanocrystals with acid hydrolysis [13, 14].

2.1.2.1 Acidic treatment on cellulose

As cellulose pulp is subjected to acid, it begins to breakdown. The fiber's most accessible regions will degrade first, then the decreasing end groups and crystal surface. Acid concentration, reaction duration, and reaction temp considered few of the significant factors to optimize acid hydrolysis of wood pulp.

The long reaction period will completely undergo hydrolysis to the cellulose crystals, but short time for reaction will result in an elevated polymerization degree (DP) due to the big, undispersed fibres. The temperature of reaction and time are related, and the greater the temperature, the shorter time needed for reaction. Nanocellulose properties are regulated not only by time and temperature, additionally by concentration of acid and acid to pulp ratio [15]. Following hydrolysis and dialysis purification, small crystalline rod-like fragments are produced into aqueous medium. When stabilized, that monocrystalline cellulose produced by acidic treatment has colloidal features and produces an aqueous dispersion. The critical concentration for the colloidal dispersion, defined as minimum concentration at which whiskers self-colloid, is influenced by size of particles, acidic processing, production conditions, aspect ratio, and ionic strength [16]. At the critical concentration of microcrystals from bleached wood pulp naturally formed as crystalline phase [17]. That have been seen for cotton cellulose whiskers, with the critical concentration in the range of 2 wt% to 10 wt% depend on the pre-production procedures. Sulfuric acid (H_2SO_4) is widely employed acid in chemical hydrolysis of nanocellulose, however other acids can also be utilised. Hydrochloric acid (HCl), hydrobromic acid (HBr), and phosphoric acid (H_3PO_4) all are applied in CNC production; however, unlike sulfuric acids, hydrochloric acid, and hydrobromic acid, they possess no surface charges, making it more difficult to generate a stable colloidal suspension. Phosphoric acid forms charged phosphate groups on the surface of nanocrystal. In production sector, sulfuric acid will be the best option of acid than hydrochloric acid.

2.1.2.1.1 Isolation of CNC by sulfuric acid

Several researchers have optimized the sulfuric acid hydrolyze reaction, and one particular method for obtaining CNC from sulfuric acid is through utilizing 64 wt% sulfuric acid solution in temperature about 45 °C within 45-60 min and continuous stirring, then cooling the matrix with 10-fold deionized water, undergoing centrifuge, followed by dialysis with deionized water till a neutral pH is obtained. For obtaining distinct crystals, that matrix must be sonicated continuously [13].

2.1.2.1.2 Isolation of CNC utilizing alternative acids

Instead of sulfuric acid, other acids, like hydrochloric acid, can be used to hydrolyze cellulose fibres into CNC. The pulp was hydrolyzed by 30 ml/g of 4 N hydrochloric acid at 80 °C for 225 minutes. The suspension is centrifuged several times till pH become 4, the non-precipitated CNC, and the supernatant became turbid. Before sonicating to disperse the suspension, the supernatant is obtained, filtered, and neutralized through

dialysis using deionized water [18]. Two additional acids that are utilized in the production of CNC are hydrobromic acid and phosphoric acid. MCC was treated with 40 ml/g 1.5-2.5 M hydrobromic acid to produce HBr-CNC.

2.1.3 Bacterial Nanocellulose (BNC)

Bacterial nanocellulose (BNC) is the final type of nanocellulose to be reviewed. It is formed by specific bacteria that produce nanofibers with nanometeric diameters and up to micromeres long. There are numerous studies and literature reviews that describe BNC structure and properties. Bacterial cellulose, against other cellulose sources, is produced in a medium for cultivation by particular bacteria such as *Acetobacter sp*. Bacteria make BNC by generating cellulose and forming bunches of microfibrils [19].

Acetobacter is a bacteria found almost everyplace sugar biodegradation occurs in environment, and this is essential in the oxidation of ethanol to acetic acid. Acetobacter is commonly utilized in the fermentation industry to manufacture acetic acid which is useful for many fields where acetic acid is important.

BNC has distinguishing characteristics such as an exceptionally fine and clear fibre structure, an elevated polymerization degree (exceeding 8,000), and better mechanical features such as mechanical strength, biocompatibility, and water holding ability [3].

Bacterial nanocellulose's main use field is in medicinal and health care applications such as patches for injury recovery or skin irritation, or as an alternative for medicinal components like veins and arteries. Additionally application sectors where BNC could be utilized in food manufacturing, packaging and paper products industries [20].

The bacteria were cultured in a medium for 3 days before being released by washing the synthesized sheet by water and utilized to generate cellulose from Acetobacter species. The cells were centrifuged and resuspended in the controlled medium. [19]. Bacterial cellulose has length of micrometer like threads in bands of nanofibrils that could be hydrolyzed to nanocrystals using, for example, sulfuric acid.

The disadvantages of BNC include the lack of bacterial cellulose, the ineffective technique of producing bacterial cellulose, and the large costs, which make commercialization difficult. The current method for synthesizing BNC cannot generate the mass amounts required for BNC commercialization, and further process improvement is required for large-scale bacterial cellulose manufacture [21].

2.2 Agricultural and bio-residues

Although wood is a main origin of CNFs, rising demand from the papers, architectures, and furniture manufacturers has raised the demand for inexpensive raw materials such as agricultural wastes as well as seasonal crops. Those compounds are regarded as a viable substitute cellulose resource to produce CNFs with suitable characteristics. Furthermore, industrial bio-residue is another by-product with significant potential for usage as a low-cost and acceptable resource for nanocellulose manufacturing. Several studies have suggested utilizing seasonal plants like linen, frill, kenaf, and agricultural outputs such as rice, sugarcane, pineapples, and wheat for this purpose. When crop residues are compared to wood, they have advantages such as reduced lignin and hemicellulose contents. Industrial bio-residue is another non-wood source that could be utilized to produce nanocellulose. In fact, as compared to other cellulosic feedstocks, industrial bio-residues have lower costs. In contrast, in a progressively eco-friendly environment, the utilization of bio-residue as another valuable material can help industry solve discard issues. These industrial bio-residues are currently either burned or utilized to low-value materials like feedstuffs. As a result, developing new value-added products from these bio-residues, like nanocellulose materials, is a viable avenue to improving the agro – environmental resources values.

Several research have been done to isolate CNFs from non-wood and bio-residue supplies such as kenaf and bast [22].

2.3 Sea animals

Tunicin, also commonly referred to as animal cellulose, is composed of very crystallized nanofibers (almost pure). The tunicate nanofiber composition, with a helical organization, differs from those found in agro-sources. [23]. Due to its significant rigidity, large dimension ratio, and outstanding interaction with suspension materials, this kind of cellulose fibril has attracted attention as a viable support for composite materials. Chemical treatment was used to produce a colloidal suspension of nanocellulose in tunicate water. To summarize, tunicate snails were chopped into tiny parts and bleached in stages. Following that, acid hydrolysis can be utilized to extract nanocellulose from bleached samples. [24]. varied acid hydrolysis conditions were used by many researchers. As, tunicate hydrolysis by 64 wt% H_2SO_4 with temperature 50 °C within 5 h, and 960 ml of H_2SO_4 98% in a 600 ml tunicate-water mixture at 60 °C for 20 min [25].

3. Characterization of nanoparticles

Several characterization methods have been utilized to analyze the different physicochemical features of NPs. Examples of those methods are X-ray diffraction (XRD), X-ray photoelectron spectroscopy (XPS), infrared (IR), scanning electron microscopy (SEM), transmission electron microscopy (TEM), Brunauer-Emmett-Teller (BET), and particle size analysis**.**

3.1 Morphological characterizations:

Morphological characteristics for NP are usually of significant concern because they influence most NP features. The most important morphological characterization methods are microscopic approaches like polarized optical microscopy (POM), scanning electron microscopy (SEM), and transmission electron microscopy (TEM). SEM approach is relied on the electron scanning principle and gives all necessary data about NPs at the nanometric scale. There is a great deal of literature describing how people employed this method to investigate not just the morphology of the nanomaterials, as well as

the suspension of nanoparticles in the mixture. Similarly, because TEM is relied upon the electron transmittance principle, which could give data on bulk materials at magnifications ranging from relatively low to extremely high.

Plant fibres, wood fibres, and other cellulosic fibres are made up of numerous interconnected cell walls. It is generally assumed that mechanical as well as chemical treatments have an effect on fibre morphology in both of diameter and quality. Microscopy studies reveal that raw wood and non-wood fibre bunches were formed up of individualized microfibers that are bound with lignin. As a result, chemical pretreatments are necessary to minimize the size of the fibre packs and the surface roughness. Many research on fibre morphology before and after chemical treatments through nanocellulose separation have been performed. The findings reveal that chemical treatments reduced the size of the fibres, and that these treatments influenced the isolation of individualized microsized fibres from fibre bundles. This is due to the elimination of certain noncellulosic constituents like as hemicellulose, lignin, and waxes.

Microscopic examination reveals CNFs separated from many resources have a web-like framework and are shaped like tangled fibrils. (Fig. 2). Tables 1 and 2 demonstrate diameter ranges of nanocellulose according to different origins. CNFs have significant differences, but CNCs have nearly similar diameters. CNF bundles can have diameters between 20 and 200 nm, according to the source, whereas individual CNFs typically have sizes between 3 and 20 nm.

Table 1. Diameter of cellulose nanofibers from various sources

Source (Cellulose nanofibers)	Diameter (nm)	References
Bacterial cellulose	40–70	[26]
Bagasse	5–15	[27]
Rice straw	4–13	[27]
Soy hull	20–120	[28]
Wheat straw	10–80	[28]

Table 2. Diameter of cellulose nanocrystals from various sources

Source (Cellulose nano-crystals)	Diameter (nm)	References
Rice straw	30.7	[29]
Bamboo	8 ± 3	[30]
Kenaf bast	2–5	[31]

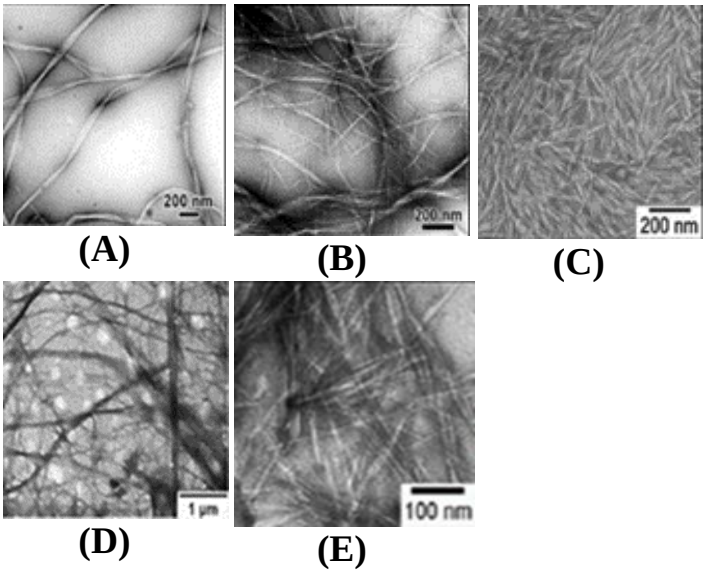

Fig. 2: Transmission electron microscope (TEM) images of isolated cellulose nanofibers, obtained from **(A)** bacterial cellulose, **(B**) banana rachis, **(C)** rice straw, **(D)** oil palm, **(E)** kenaf bast [32 – 36].

Regardless of the origin of cellulose nanofibrils, the influence of treatments on its morphological structure is a significant consideration. The cycle time of cellulose mixtures in mechanical equipment is another feature which could influence the morphology and structure of cellulose nanofibers. A diameter of fibers varied from submicron to nanoscale as the number of cycles increased from one to five. Furthermore, it was mentioned that, despite the material source, previous treatment and hydrolysis conditions are essential determinants in defining CNC dimensions, underlining the idea that pulp is not required to separate cellulose nanocrystals from raw cotton linter [32].

3.2 Structural characterizations

While researching the composition and type of bonding materials, structural properties are essential. Structural characteristics give much information for the subject material's bulk characteristics. The most generally utilized approaches for studying the structural properties of NPs involve XRD, energy dispersive X-ray (EDX), XPS, IR, Raman, BET, and Zieta size analyzer.

XRD is an essential approach to identify the structural features of nanoparticles. X-ray diffraction investigations of nanocellulose fibres that are based on periodic arrays of atoms, were used due to variety of reasons, including identifying the H-bond, refining atomic positions, and determining the crystallinity degree [33].

X-ray diffraction (XRD) is commonly employed to study the crystalline structure of lignocellulosic materials. It is generally known that cellulose has a molecular structure that is part crystalline and part amorphous [34]. This means that mutual H-bonding bonds the cellulose chains tightly together through the crystalline (ordered) areas, while weaker H-bonding occurs within the amorphous (disordered) regions of cellulose [35].

The X-ray diffraction technique, in association with other procedures (NMR and 380-Raman), can measure the comparative crystallinity value for primary cellulosic materials and derivatives. Many parameters, including the origin of cellulose, extraction technique conditions, and pretreatments, influence crystallinity of nanocellulose in crystalline and fibre structure. like, the crystallinity for linen, squash, and wood CNFs is found to be 59, 64, and 54%, respectively, [36] whereas CNCs from sisal, rice husk, flax, cotton, maize and commercial MCC were estimated to be 85.9, 76, 84.9, 94, 80.6, and 81.7% [37].

XPS is the most sensitive technology for detecting the actual elemental ratio and bonding type in components in nanoparticle substances. XPS is surface accurate approach that could be utilized in depth profiling research to figure out the whole composition and composition changes in depth. XPS is dependent on fundamental spectroscopic concepts, and a standard XPS spectrum is a plot with the number of electrons on the Y-axis versus the electron binding energy (eV) on the X-axis. Every element possess a unique fingerprint binding energy value, resulting in a distinct sequence of XPS peaks.

FT-IR and Raman spectroscopies are often utilized in analyzing the vibrational properties of nanoparticles. When compared to other elemental analytical techniques, these seem to be most developed and efficient. The fingerprint band, which gives material signature information, is the most important range for NPs.

3.3 Thermal characterizations

Cellulosic materials are renowned because of their rapid thermal decomposition at lower to medium temperatures, specifically under 400oC [38]. Hemicellulose decomposition is the first step in the thermal decomposition of lignocellulosic materials, then lignin pyrolysis, cellulose depolymerization, active flame combustion, and char oxidation [39]. When the manufacturing temperature for thermoplastic polymers surpasses 200oC, the thermal stability of cellulosic fibres must be investigated to determine their suitability for composite technology. Because the thermal decomposition of cellulose fibres is significantly affected with their composition and chemical constitution, different cellulosic fibres have various decomposition profiles. According to latest studies, larger extractive contents, when combined by reduced crystallinity and lower crystal size, can promote thermal degradation and lower thermal stability of lignocellulosic fibres [40]. Many investigations on the thermal stability of cellulosic fibres and nanocelluloses have been performed (Table 3).

Recent research has shown that CNFs have significant thermal characteristics, which made them attractive candidates for thermoplastic composites. The greater degradation onset temperature reported for CNFs reflects the fibers' enhanced thermal behavior. This is because hemicellulose, pectin, and lignin were removed out of suspension through the nanofiber separation procedure.

Table 3: Thermal characterization of nanocellulose from different origins after selective chemical pretreatments.

Materials	Onset of degradation (°C)	Main degradation step (°C)	Ref.
Sugarcane bagasse (Bleached)	270		[41]
Sugarcane bagasse (Crystals (30 min hydrolyzed)	255		
Sugarcane bagasse (Crystals (75 min hydrolyzed)	210		
Kenaf (Raw bast)	177	321	[42]
Kenaf (NaOH treated fibers)	256	368	
Kenaf (Bleached fibers)	220	346	
Kenaf (Sulfuric acid crystals)	171	317	
Kenaf (HCl crystals)	256	358	
Soy hulls (Initially (raw)	190	327	[43]
Soy hulls (Treated after the purification)	240	342	
Soy hulls (Crystals)	170	294	

4. Different methods for sensor immobilization on substrate

Immobilization is defined as any activity that stops or prevents anything or someone from moving freely or working effectively as it does. An act of immobilization, for example, is stopping a moving vehicle. Hence, immobilization can be thought of as a technique for stopping an agent by utilizing an appropriate immobilizer.

Immobilization is a branch of research that focuses on enzyme, cell, molecule, and even atom immobilization using many types of ancient and new immobilizer materials. The immobilization research also focused at novel technology, technique, preparation, application, analysis, and knowledge regarding the interaction between the immobilizer and its immobilization agent. Immobilization research began in the 1916-1940s, and it grew tremendously over the next four decades, being defined as underdeveloped, growing, developed, post-development, and now in the exciting period of the twenty-first century (2). In the twenty-first century, the most advanced, sophisticated, and complex immobilization methods have been investigated. The discovery of nanotechnology has significantly advanced research and development in immobilization technology. The fact that smaller molecules can be detained and manipulated opened new avenues for dealing with them and solved an age-old difficulty in immobilization that had previously plagued researchers.

4.1 Types of Immobilizations

Immobilization is the result of the interaction of two entities: an immobilizer and an immobilization agent [44] The immobilization preparation process is determined by both entities' ability to react and generate a stable and suitable immobilized phase. An immobilized system is ready to achieve its specific goal, such as obtaining sustaining immobilization, increasing agent recyclability, agent purification, or process control [45].

4.1.1 Physical immobilization methods

Physical immobilization is the first type of immobilization, and it was developed primarily for protein isolation [36]. It primarily includes physical interaction in which neither the immobilizer nor the immobilization agent are modified, bonded, or changed in order to immobilize them. Physical immobilization strategies include encapsulation, entrapment, or confinement; adsorption; and non-covalent contact [46]

4.1.1.1 Encapsulation and entrapment

An encapsulation method can be described to enclose or surround the immobilization agent inside a vesicle of a nano-capsule structure made of suitable vesicle-forming immobilizer biomaterial. On the other hand, in the entrapment or confinement method of immobilization, agents are either trapped or suspended in the nano-sphere particle or nano-crystal lattice, which are inert to the agent itself. The method is dependent on the environment, and the intermolecular forces generated are weak (electrostatic, hydrophobic, van der Waals, hydrogen bonds).

4.1.1.2 Adsorption

Adsorption is the adhering of atoms, ions, or molecules of gas, liquid, or melted solids to a surface. This is achieved through non-covalent interactions between sensing molecules and surfaces such as electrostatic, Vander Waals, hydrophobic, and so on. The adsorption method's technique is the simplest [47].

Immobilized agents can be adsorbed naturally on the external or internal surface of a biomaterial in the form of non-specific binding. The non-specific binding of electrostatic or hydrophobic affinity is weak, temporary, and easily removed by another strong competing agent.

Adsorption immobilization can be performed by a static process, a dynamic batch process, a reactor loading process, or an electrode position process. The selection of adsorption preparation methods depends on the high yield of agent adsorption and the high activity of the agent. In the static process, an agent is immobilized on material by running its solution on the immobilized surface without stirring to allow gentle and natural absorption. The dynamic batch process added continuous stirring and agitating between the immobilizer solution and the agent solution. During the reactor loading process, an agent solution will be added to the reactor and agitated. Lastly, the electrode positioning process utilizes an electrode-loaded immobilizer, which becomes the depositing surface of the migrating agent [48].

In a while, the comparative weakness of adsorptive binding forces is a disadvantage. Adsorbed compounds are desorbed in an easy way by changes in temperature, and as well as by modifying the substrate and ionic concentrations. As a result, when using biocatalysts immobilized by adsorption, special attention must be taken to maintain stable reaction conditions.

4.1.2 Chemical immobilization methods

Chemical reactions are used in the procedures for chemical immobilization to produce a high strength bond between both entities. The immobilizer is either covalently or crosslinked to the immobilization agent's molecule due to such a chemical reaction, depending on the type of bond produced. Immobilization resulted from covalent bonding when particular covalent bonds were formed between both entities and electron sharing was included. Cross-linking happens when an intermediate forms covalent or ionic bonds between two entities that are far stronger than covalent bonds and provide greater stability and immobilization time.

When significant recovery and recyclability of the immobilized agent and target material are required, chemical immobilization is particularly advantageous. This is because this method provides extremely powerful immobilization and protection for the entities against loss and leaks. Furthermore, its preparation is costly, time-consuming, and intricate.

4.1.2.1 Covalent bond

Unlike non-covalent interaction, covalent bonding is advantageous because pH ranges, ionic strength, non-specific bonding, and leakage problems do not affect them. However, the immobilized agent's active site may be lost if the covalent bonds formed at the active site destroy its function. A suitable covalent bonding site should be investigated on the agent, which is rather difficult for a new and unknown agent. Additionally, known active agents can also be protected prior to immobilization. It involves complicated preparation and is expensive [49].

4.1.2.2 Cross-linking:

Cross-linking of an agent for immobilization involves covalent bonding and intermediary linkers between the immobilized surface and the immobilizer agent. The linkers act as a polymerization agent added to the preparation to provide the required linkage of surface and agent [40]. Like covalent bonding, cross-linker immobilization is not affected by pH or ionic strength. Furthermore, it has no effect on immobilized agent activity, resulting in higher agent activity than covalent bonds.

The most often utilized cross-linker in immobilization preparation is glutaraldehyde. Additional cross-linkers utilized to polymerize biomaterial surfaces for agent immobilization include hexamethylene, diisocyanate, difluoro-dinitrobenzene, and dimethyl suberimidate.

Therefore, the physical immobilization method presents several advantages over the chemical immobilization method. First, it preserves the purity and function of the immobilization agent, which means that the agents are highly active and did not interact with the immobilizer prior to action. The releasing of agents is more rapid, natural, and gentle because no strong bonding interactions existed

and were required to be disassociated. Finally, its preparation is also much easier than the other methods, generally, no special chemical is required to form the immobilization steps. This method is natural and very organic in its development and application.

However, the advantage of physical immobilization is also its drawback. The undisruptive interaction of biomaterial and immobilized agent provides only a weak adsorption force; thus, it is easily detached. Harsh environments and interferences can easily dissociate weak non-covalent interactions. Consequently, agent leakage and loss may occur between preparation and application. Additionally, the noncovalent interaction is also non-specific to the target agent and may adsorb other unwanted agents or competing agents.

5. Typical optical sensing strategies

5.1. Fluorescence sensing strategy:

Haq Nawaz et al. created a multifunction cellulose-based intelligent luminescent material (Lum-MDI-CA) that possess an extensive conjugation structure, which used to identify Cu^{2+} and Fe^{3+} ions in a quick, sensitive, and dual mode. The sensor performed outstandingly in terms of detecting and removing Cu^{2+} ions and Fe^{3+} ions [50].

Rhodamine B is a widely utilized xanthene-family luminous dye, and their derivatives are generally applied as fluorescent chemosensors because of its distinctive photophysical properties.

Wang et al. developed a naphthalimiderhodamine B derivative 1 for fluorometric as well as colorimetric detecting for Sn^{4+}, Cu^{2+} and Cr^{3+} ions [51].

Vanshika et al. developed a new quinazolin-based Schiff base chemosensor (E)-2-benzamido-N-(1-(pyridin-2-yl)ethylidene) benzohydrazide (L). The receptor showed a significant colorimetric wavelength change in the presence of both Ni^{2+} and Zn^{2+} ions, as well as a fluorometric "turn on" reaction in the existence of Zn^{2+} ion only [52].

Flavones framework (3-hydroxyflavone (3HF)) was designed by *Nisha et al.* 3HF showed great sensitivity and selectivity in both colorimetric and fluorescence (FL) turn-off responses to Cu^{2+} and Fe^{2+}. Meanwhile, naked-eye detection is provided by the distinct color change and quick quenching of FL intensity [53].

Adhikari's group created a ratiometric fluorescent chemosensor for Sn^{2+} sensing based on the sensing technique of Sn^{2+}-induced spirocyclic ring opening of the rhodamine molecule. The free probe first appeared to have an absorption max at 323 nm in a 1:4 acetonitrile: HEPES (10 mM, pH 7.4) solution. A band of absorption at 323 nm reduced as Sn^{2+} was gradually added, while the band of absorption at 556 nm increased, as a result, there are observable colour shifts from colourless to pink. Nevertheless, when Sn^{2+} was added to the probe mixed solution, the first emission band at 442 nm was reduced then novel band emerged at 599 nm (red-shifted by 157 nm, ex = 366 nm), as a result of the Sn^{2+} driven spirolactam ring opening of the rhodamine entity [54].

Vinod Kumar Gupta et al. used a simple refluxing procedure to create two novel significantly selective colorimetric and fluorogenic amino pyridine Schiff bases (L1 and L2), which are then analyzed using typical NMR and HRMS methods. Its superior metal detection capabilities were investigated using absorbance and fluorescence spectroscopy. The colorimetric detecting activity of probes L1 and L2 towards Ni(II), Zn(II), Fe(III), and UO2(II) ions was thoroughly examined, through many elements of sensing activity as sensitivity, binding constant, stoichiometry, pH range, and interference effect being carefully investigated. Furthermore, L1 and L2 showed outstanding "off-on" fluorogenic selectivity with Zn (II). The findings show how sensors functioned well in colorimetric also in fluorogenic detecting under neutral conditions, in a lower limit of detection [55].

Min Wu et al. created a multiple bonding site chemosensor, N-(3-methoxy-2-hydroxybenzylidene)-3-hydroxy-2-naphthahydrazone (H_3L). It could sense Cd^{2+} and Zn^{2+} ions in a selective way in the "off-on" mode dependent on the AIE of their complexes in THF/HEPES and THF/H_2O media, providing novel technique for AIE-based target sensing. Zn^{2+} and Cd^{2+} detection limits are 9.85 10-9 M and 1.27 10^{-7} M. The chemosensor combines with the Cd^{2+} and Zn^{2+} ions with various formation and combination ways, resulting in the emission position of the aggregates at 560 and 645 nm, respectively, from which Cd^{2+} ions were effectively distinguished from Zn^{2+} ions [56]

Hafiz Muhammad Junaid et al. created Fluorenone-based fluorescent and colorimetric sensors 1 and 2 that detected iodide ions selectively in the presence of interferences. The fluorescence emission improvement response towards I was proved by sensors with detection limits of 8.0 and 11.0 nM, obtained by inhibiting intramolecular charge transfer and C-N double bond isomerization [57].

R. Bhaskar et al. created a successful fluorescence sensor dependent on thiocarbohydrazide S5 for the selective measuring for Hg^{2+} within semi-aqueous medium. When Hg^{2+} was added to the sensor S5, it changed color and turned off the fluorescence. The detection limit for Hg^{2+} was reported as 1.26 nm [58].

Puthiyavalappil Rasin et al. used a simple Schiff base reaction to create PyAP [(Z)-2-((pyren-1-ylmethylene) amino) phenol], a pyrene-based fluorescence sensor. Only Ga^{3+} ions are detected by the PyAP fluorescence chemosensor with the influence of other metal ions. Moreover, PyAP proved excellent selectivity and sensitivity for the detection of Ga^{3+}. 3.35 nM was the detection limit. The detection limits were 3.35 nM. The chemosensor PyAP is dependent on the photo-induced electron transfer (PET) mechanism [59].

Sungjin Moon et al. designed DiPP ((E)-3-(4-(diphenylamino) phenyl)-1-(pyridin-2-yl) prop-2-en-1-one), the fluorometric also colorimetric chemosensor relying on a chalcone structure with a triphenylamine group. Pd^{2+} is detected by DiPP with fluorescence turned off and colorimetry ranging from yellow to purple. The binding ratio

of DiPP to Pd^{2+} was observed to be 1:1. The fluorescence and colorimetric detection limits for Pd^{2+} by DiPP were determined to be 0.67 M and 0.80 M, respectively [60].

5.2 Colorimetric sensing strategy

Lei Wang et al. developed a new cellulosic colorimetric sensor (DAC-Tu) containing N and S Ag^{+} spots. In mixed metal ions aqueous solutions, the DAC-Tu shows exceptional selectivity and sensitivity for Ag^{+}, have noticeable color shift from white to black visible. The produced DAC-Tu colorimetric sensor shown remarkable application potential for in-situ human eye detection of Ag^{+} [61].

Fasil et al used microwave irradiation to design and synthesize a new sensor (RD) containing rhodamine B and 4-tert-Butyl phenol. The sensor detects Cu^{2+} selectively by developing an absorptive compound and initiating the synthesis of a luminously colored ring-open spirolactam. The sensor's recognition capability was analyzed using absorbance and infrared measurements (IR) [62].

Patil et al produced a Schiff base based on benzohydrazide with condensation of 2-amino-quinoline-3-carbaldehyde and 4-nitrobenzohydrazide. In CH_3CN solution, the colorimetric detecting activity of Schiff base ligand (SBL) towards different metal ions is effectively examined. The wavelengths changed significantly after the addition of Cu^{2+} [63].

Thit Pipattanawarothai et al. create a recyclable, selective and colorimetric chemosensor for ferric ion identification by naked eyes (rhodamine-based chelator) (RB-UTES). The structure and sensing properties of RB-UTES are studied. The chelator was ferric ion sensitive and selective, and it form covalent bond with poly (vinyl alcohol) via a siloxane linkage generated by the sol-gel reaction. The free-standing sensor film showed excellent selectivity and sensitivity to ferric ion by simply soaking in aqueous solutions, allowing visual detection with significant formation of pink hue through the film. The sensor film can be returned to its first color by washing with 0.1 M ethylene diamine, providing several detection cycles [64].

Jae Sung Heo et al. developed a colorimetric chemosensor BHSO ((Z)-30,60-bis (diethylamino)-2-(((For detecting Cu^{2+}, use 8-hydroxy-2,3,6,7-tetrahydro-1H,5H-pyrido[3,2,1-ij]quinolin-9- yl) methylene) amino) ethyl) spiro [isoindoline-1,90-xanthen]-3-one). BHSO made color transform from colorless to vivid orange in the existence of Cu^{2+}. The detection limit for Cu^{2+} towards BHSO is 0.73 M. UV-vis titrations were used to prove the binding property of BHSO and Cu^{2+}. When Cu^{2+} was added to BHSO, the absorbance at 476 nm elevated to 1.4 equivalents of Cu^{2+}. A sound isosbestic point of 366 nm indicated that BHSO had reacted with Cu^{2+} to form compounds [65].

Chang Joo Rha et al. developed the ATAMsal ((E)-3-((2-hydroxy-3-methoxybenzylidene) amino) thiophene-2-carboxamide) colorimetric chemosensor for sensing Cu^{2+} and Co^{2+} in solution. The ATA-Msal sensor could detect Cu^{2+} and Co^{2+} through changing color from colorless to pale yellow. ATA-Msal detection limits for Cu^{2+} (0.14 M) and Co^{2+} (0.88 M) [66].

Dhanushkodi Mohanasundaram et al. developed a new pyridine-based receptor (S) for the selective sensing of copper ion in presence of various metals. Colorimetry, absorption, and emission spectroscopy systems in CH3CN/H2O (7:3, v/v) were used to study the metal detecting capability of receptors with various metal ions. In ordinary light and UV light with copper ion, that receptor exhibits a significant color shift from colorless to yellow and cyan. Furthermore, upon excitation at 388 nm, the S-Cu^{2+} complex gives a novel UV-Visible band at 419 nm and a strong fluorescence band at 494 nm [67].

Greeshma Gigi et al. created a portable solid-state opto-sensor that is aqua-compatible and visible for the naked eye for the selective and sensitive sensing for ultra-trace Hg^{2+} ions. A chromoionophoric probe formed from 2,3-bis((4-isopropylbenzylidene) amino) maleonitrile (PDPM) was directly impregnated into the surface of a structurally designed porous polymer monolithic framework to create proposed chemosensor. After complexing with Hg^{2+}, the sensor produced a remarkable color change from white to yellow. The monolithic sensor performed best at pH 8.0, with quick signal response kinetics of 60s and a broad linear response (0.5-150.0 g/L) with detection limit of 0.22 g/L. Additionally, that sensor is resistant to foreign matrix constituents, allowing it to detect Hg^{2+} with great precision [58].

Hyejin Nam et al. created a dinitrophenol-based colorimetric chemosensor that detects Cu^{2+} and S^{2-}, HDHT ((E)-2-(2-(2-hydroxy-3,5-dinitrobenzylidene)hydrazineyl)-N,N,N-trimethyl-2-oxoethan-1-aminium). The HDHT sensed Cu^{2+} by transformation of its color from yellow to colorless. The HDHT detection limit for Cu^{2+} is counted to be 6.4 10-2 M. The HDHT isn't significantly influenced by different metal ions in its detection of Cu^{2+} in the interference test [69].

5.3 Other detecting strategies

Ujjal Haldar et al. designed a water-soluble polymeric probe which could be utilized for the colorimetric sensing to cyanide ions within aqueous solutions. Particularly, P1, water soluble random terpolymer (P1) of N,N dimethylacrylamide, 2-((E)- 4-((E)-(4-((2 (acryloyloxy) ethyl) (methyl) amino) phenyl) diazenyl) styryl)-1,3,3-trimethyl-3H-indol-1-ium (M1), and N-(4-benzoylphenyl)acrylamide have been prepared by free-radical polymerization. M1 showed significant CN^{-}detection capability in EtOH-HEPES buffer solution, with low LOD value of 0.36 M and a significant colour change from brick red to yellow caused by the ICT process shutdown. P1, a polymeric probe based on M1, showed high selectivity and sensitivity (LOD = 1.23 μM) for the detection of CN^{-} in aqueous HEPES buffer solution [70].

Tianlei Qin et al. present a new technique for multi-detection for metal ions by a carbon quantum dots (CQDs)-based chemosensor array, in which the CQDs are worked through many amino acids (glutamine, histidine, arginine, lysine, and proline), that was acting for detecting elements in the sensor array. The designed chemosensor array successfully recognizes eleven metal ions with 100%

classification accuracy. Notably, the suggested approach used a support vector machine to measure the concentration of specific metal ions in the matrix(SVM). The sensor array also allows for the qualitative detection of unidentified metal ions in presence of ordinary water. As a result, the method offers unique high-throughput approach for identifying different analytes in complex systems [71].

C.W. Ooi et al. used an L-Cysteine functionalized gold-coated tilted fibre Bragg screen to detect metal ions (Au-TFBG). L-cysteine (L-cys) is a semi-essential amino acid with a good ability to create Au-S bonds on the gold surface of the sensor via thiol group, while the amine and carboxyl groups in the L-cys molecules could act like ligands which link with the metal ions in mixture. Results show that the sensor is selective and sensitive to various metal ions such as Co^{2+}, Cd^{2+}, Cu^{2+}, Pb2+, Ni^{2+}, and Zn^{2+}. The selectivity test indicates how the sensor has a strong affinity for the metal ion Cu2+, with a reported LOD of 0.19 M [72].

Using a one-pot multiple processes synthesis technique, *Muhammad Mansham et al.* created a chemosensor by covalently attaching naphthalene to silicon nanoparticles (NSPs). Photoluminescence (PL) spectroscopy was used to examine the NSPs as a chemosensor to sense Hg^{2+} ion in water samples. The findings show that the fluorescence characteristics of NSPs (20 ppm) were quenched by Hg^{2+} addition in the 0 to 50 ppm range. The NSPs chemosensor linearity within 5 - 1000 ppb as well as a limit of detection LOD (1 ppb; 5 nM) [73].

Battal, A., Kassa, S.B., Gultekin, N.A. et al. created a new carbazole-based chemosensor from 2-(N-hexylcarbazol-3'-yl)-pyridine-5-carbaldehyde that called probe 7b. The probe 7b is more sensitive to the Fe^{3+} ion than to other interferences. Probe 7b's selectivity and reactivity to Fe^{3+} were extremely suitable for usage in applications. The limit of detection (LOD) value for probe 7b is determined to be 1.38 nM. The value was extremely low in comparison to its analogues in the literature [74].

References

1- Moon, R. J., Martini, A., Nairn, J., Simonsen, J., & Youngblood, J. (2011). Cellulose nanomaterials review: structure, properties and nanocomposites. Chemical Society Reviews, 40(7), 3941-3994.

2- Moon, R. J., Frihart, C. R., & Wegner, T. Nanotechnology applications in the forest products industry. Forest products journal, 56 (5) (2006) 4-10.

3-Kamel, S. Nanotechnology and its applications in lignocellulosic composites, a mini review. Express Polymer Letters, 1(9) (2007) 546-575.

4- Klemm, D., Kramer, F., Moritz, S., Lindström, T., Ankerfors, M., Gray, D., & Dorris, A. Cellulose Nanocrystals: Chemistry, Self-Assembly, and Applications. Angew. Chemie-Int. Ed, 50(24) (2009) 5438-5466.

5- TAPPI's International Nanotechnology Division. Roadmap for the Development of International Standards for Nanocellulose [Report]. October 2011.

6- Bledzki, A. K., & Gassan, J. Composites reinforced with cellulose based fibres. Progress in polymer science, 24(2) (1999) 221-274.

7- Mohanty, A. K., Misra, M. A., & Hinrichsen, G. I. Biofibres, biodegradable polymers and biocomposites: An overview. Macromolecular materials and Engineering, 276(1) (2000) 1-24.

8- McCann, M. C., Wells, B., & Roberts, K. Direct visualization of cross-links in the primary plant cell wall. Journal of cell science, 96(2) (1990) 323-334.

9- Dinand, E., Chanzy, H., & Vignon, R. M. Suspensions of cellulose microfibrils from sugar beet pulp. Food hydrocolloids, 13(3) (1999) 275-283.

10- Dufresne, A., Cavaillé, J. Y., & Vignon, M. R. Mechanical behavior of sheets prepared from sugar beet cellulose microfibrils. Journal of applied polymer science, 64(6) (1997) 1185-1194.

11- Azizi Samir, M. A. S., Alloin, F., & Dufresne, A. Review of recent research into cellulosic whiskers, their properties and their application in nanocomposite field. Biomacromolecules, 6(2) (2005) 612-626.

12- Håkansson, H., & Ahlgren, P. Acid hydrolysis of some industrial pulps: effect of hydrolysis conditions and raw material. Cellulose, 12(2005) 177-183.

13- Dong, X. M., Revol, J. F., & Gray, D. G. Effect of microcrystallite preparation conditions on the formation of colloid crystals of cellulose. Cellulose, 5(1998) 19-32.

14- Angellier, H., Molina-Boisseau, S., Lebrun, L., & Dufresne, A. Processing and structural properties of waxy maize starch nanocrystals reinforced natural rubber. Macromolecules, 38(9) (2005) 3783-3792.

15- Orts, W. J., Shey, J., Imam, S. H., Glenn, G. M., Guttman, M. E., & Revol, J. F. Application of cellulose microfibrils in polymer nanocomposites. Journal of Polymers and the Environment, 13(2005) 301-306.

16- Pitkänen, M., Honkalampi, U., Von Wright, A., Sneck, A., Hentze, H. P., Sievänen, J., ... & Hellen, E. Nanofibrillar cellulose: In vitro study of cytotoxic and genotoxic properties. In 2010 TAPPI International Conference on Nanotechnology for the Forest Product Industry (pp. 246-261) (2010). TAPPI Press.

17- Revol, J. F., Bradford, H., Giasson, J., Marchessault, R. H., & Gray, D. G. Helicoidal self-ordering of cellulose microfibrils in aqueous suspension. International journal of biological macromolecules, 14(3) (1992) 170-172.

18- Araki, J., Wada, M., Kuga, S., & Okano, T. Flow properties of microcrystalline cellulose suspension prepared by acid treatment of native cellulose. Colloids and Surfaces A: Physicochemical and Engineering Aspects, 142(1) (1998) 75-82.

19- Tokoh, C., Takabe, K., Fujita, M., & Saiki, H. Cellulose synthesized by Acetobacter xylinum in the presence of acetyl glucomannan. Cellulose, 5(1998) 249-261.

20- Geyer, U., Heinze, T., Stein, A., Klemm, D., Marsch, S., Schumann, D., & Schmauder, H. P. Formation, derivatization and applications of bacterial cellulose. International Journal of Biological Macromolecules, 16(6) (1994) 343-347.

21- Czaja, W., Krystynowicz, A., Bielecki, S., & Brown Jr, R. M. Microbial cellulose—the natural power to heal wounds. Biomaterials, 27(2) (2006) 145-151.

22- Jonoobi, M., Mathew, A. P., & Oksman, K. Producing low-cost cellulose nanofiber from sludge as new source of raw materials. Industrial Crops and Products, 40(2012) 232-238.

23- Nishiyama Y, Sugiyama J, Chanzy H, Langan P. Crystal structure and hydrogen bonding system in cellulose Ia from synchrotron X-ray and neutron fiber diffraction. J AmChem Soc 125(2003) 14300–14306

24- Schroers, M., Kokil, A., & Weder, C. Solid polymer electrolytes based on nanocomposites of ethylene oxide–epichlorohydrin copolymers and cellulose whiskers. Journal of Applied Polymer Science, 93(6) (2004) 2883-2888.

25- Zhang, J., Song, H., Lin, L., Zhuang, J., Pang, C., & Liu, S. Microfibrillated cellulose from bamboo pulp and its properties. Biomass and Bioenergy, 39(2012) 78-83.

26- Castro C. et al Bacterial cellulose produced by a new acid-resistant strain of Gluconacetobacter genus. Carbohydr Polym 89 (2012) 1033–1037

27- Hassan M.L., Mathew A.P,. Hassan E.A., El-Wakil N.A., Oksman KNanofibers from bagasse and rice straw: process optimization and properties. Wood Sci Technol 46.(2012) 193–205

28- Alemdar A., Sain M. Isolation and characterization of nanofibers from agricultural residues—wheat straw and

soy hulls. Bioresour Technol 99 (2008) 1664–1671

29- Lu P., Hsieh Y. L., Preparation and characterization of cellulose nanocrystals from rice straw. Carbohydr Polym 87 (2012) 564–573

30- Brito BSL, Pereira FV, Putaux JL, Jean B (2012) Preparation, morphology and structure of cellulose nanocrystals from bamboo fibers. Cellulose 19:1527–1536

31- Zaini L.H., Jonoobi M., Tahir P.M., Karimi S. Isolation and characterization of cellulose whiskers from kenaf (Hibiscus cannabinus L.) bast fibers. J Biomater Nanobiotechnol 4 (2013) 37–44.

32- Morais, J. P. S., de Freitas Rosa, M., Nascimento, L. D., Do Nascimento, D. M., & Cassales, A. R. Extraction and characterization of nanocellulose structures from raw cotton linter. Carbohydrate polymers, 91(1) (2013) 229-235.

33- French, A. D. Idealized powder diffraction patterns for cellulose polymorphs. Cellulose, 21(2) (2014) 885-896.

34- Ciolacu, D., Ciolacu, F., & Popa, V. I. Amorphous cellulose—structure and characterization. Cellulose chemistry and technology, 45(1) (2011) 13.

35- Parikh, D. V., Thibodeaux, D. P., & Condon, B. X-ray crystallinity of bleached and crosslinked cottons. Textile Research Journal, 77(8) (2007) 612-616.

36- Bhatnagar, A., & Sain, M. Processing of cellulose nanofiber-reinforced composites. Journal of reinforced plastics and composites, 24(12) (2005) 1259-1268.

37- Luduenă LN, Vecchio A, Stefani PM, Alvarez VA, Extraction of cellulose nanowhiskers from natural fibers and agricultural byproducts. Fibers Polym 14(2013) 1118–1127.

38- Hajaligol, M., Waymack, B., & Kellogg, D. Low temperature formation of aromatic hydrocarbon from pyrolysis of cellulosic materials. Fuel, 80(12) (2001) 1799-1807.

39- Lee, H. L., Chen, G. C., & Rowell, R. M. Thermal properties of wood reacted with a phosphorus pentoxide–amine system. Journal of Applied Polymer Science, 91(4) (2004) 2465-2481.

40- Ornaghi, H. L., Poletto, M., Zattera, A. J., & Amico, S. C. Correlation of the thermal stability and the decomposition kinetics of six different vegetal fibers. Cellulose, 21(2014) 177-188.

41- Teixeira E.D.M., Bondancia T.J., Teodoro K.B.R., Correâ A.C., Marconcini J.M., Mattoso L.H.C.,Sugarcane bagasse whiskers: extraction and characterizations. Ind Crops Prod 33 (2011) 63–66

42- Zaini L.H., Jonoobi M., Tahir P.M., Karimi S. Isolation and characterization of cellulose whiskers from kenaf (Hibiscus cannabinus L.) bast fibers. J Biomater Nanobiotechnol 4 (2013) 37–44.

43- Flauzino Neto W.P., Silvério H.A., Dantas N.O., Pasquini D. Extraction and characterization of cellulose nanocrystals from agro-industrial residue—soy hulls. Ind Crops Prod 42 (2013) 480–488

44- Cao, L. Introduction: Immobilized enzymes: Past, present and prospects. Carrier-bound immobilized enzymes: principles, application and design, 1 (2005) 1-52.

45- Ling, T.L., Ahmad, M., Heng, L.Y., Journal of biosensors, (2011),

46- Taranejoo S, Monemian S, Moghri M, Derakhshankhah H.Development of ultrasmall chitosan/succinyl β-cyclodextrin nanoparticles as a sustained protein-delivery system. (2013)

47- Lodish H, Berk A, Zipursky SL, Matsudaira P, Baltimore D, Darnell J. Noncovalent Bonds. W. H. Freeman; (2000).

48- D'souza SF. Immobilized enzymes in bioprocess. Current Science.(1999).

49- Taylor, R. F., & Schultz, J. S. (Eds.). (1996). Handbook of chemical and biological sensors. CRC Press.

50- Nawaz, H., Chen, S., Li, X., Zhang, X., Zhang, X., Wang, J. Q., & Xu, F. Cellulose-based environment-friendly smart materials for colorimetric and fluorescent detection of Cu^{2+}/Fe^{3+} ions and their anti-counterfeiting applications. Chemical Engineering Journal, 438 (2022) 135595.

51- Wang Q., Li C., Zou Y., Wang H., Yi T. and Huang C., Org. Biomol., 10 (2012) 6740–6746.

52- Sharma, V., Sahu, M., Manna, A. K., De, D., & Patra, G. K. A quinazolin-based Schiff-base chemosensor for colorimetric detection of Ni^{2+} and Zn^{2+} ions and 'turn-on'fluorometric detection of Zn^{2+} ion. RSC advances, 12(53) (2022) 34226-34235.

53- Fatma, N., Mehata, M. S., Pandey, N., & Pant, S. Flavones fluorescence-based dual response chemosensor for metal ions in aqueous media and fluorescence recovery. Journal of Fluorescence, 30(2020) 759-772.

54- Adhikari, S., Ghosh, A., Guria, S., & Sahana, A. A through bond energy transfer based ratiometric probe for fluorescent imaging of Sn 2+ ions in living cells. RSC advances, 6(46) (2016) 39657-39662.

55- Gupta, V. K., Singh, A. K., Kumawat, L. K., & Mergu, N. An easily accessible switch-on optical chemosensor for the detection of noxious metal ions Ni (II), Zn (II), Fe (III) and UO_2 (II). Sensors and Actuators B: Chemical, 222(2016) 468-482.

56- Wu, M., Yang, D. D., Zheng, H. W., Liang, Q. F., Li, J. B., Kang, Y., Jin, L. P. A multi-binding site hydrazone-based chemosensor for Zn (II) and Cd (II): a new strategy for the detection of metal ions in aqueous media based on aggregation-induced emission. Dalton Transactions, 50(4) (2021) 1507-1513.

57- Hafiz Muhammad Junaid, Muhammad Tahir Waseem, Zulfiqar Ali Khan, Farhan Munir, Summar Sohail, Umar Farooq, and Sohail Anjum Shahzad Fluorenone-Based Fluorescent and Colorimetric Sensors for Selective Detection of I^- Ions: Applications in HeLa Cell Imaging and Logic Gate, *ACS Omega* (2022).

58- Bhaskar, R., & Sarveswari, S. Thiocarbohydrazide based Schiff Base as a Selective Colorimetric and Fluorescent Chemosensor for Hg^{2+} with “Turn-Off” Fluorescence Responses. ChemistrySelect, 5(13) (2020) 4050-4057.

59- Rasin, P., Haribabu, J., Malappuram, K. M., Manakkadan, V., Palakkeezhillam, V. N. V., Echeverria, C., & Sreekanth, A. A “turn-on” fluorescent chemosensor for the meticulous detection of gallium (III) ion and its use in live cell imaging, logic gates and keypad locks. Journal of Photochemistry and Photobiology A: Chemistry, 437(2023) 114493.

60- Moon, S., & Kim, C. A, Fluorescent and Colorimetric Chemosensor Detecting Pd^{2+} Based on Chalcone Structure with Triphenylamine. Journal of Fluorescence, (2023)1-10.

61- Wang, L., Zhang, C., He, H., Zhu, H., Guo, W., Zhou, S., & Zhang, J. Cellulose-based colorimetric sensor with N, S sites for Ag^{+} detection. International Journal of Biological Macromolecules, 163 (2020) 593-602.

62- Abebe, F., Gonzalez, J., Makins-Dennis, K., & Shaw, R. A new bis (rhodamine)-based colorimetric chemosensor for Cu^{2+}. Inorganic chemistry communications, 120(2020) 108154.

63- Patil, D. Y., Khadke, N. B., Patil, A. A., & Borhade, A. V. Amino-quinoline based colorimetric chemosensor for Cu^{2+} detection. Journal of Analytical Chemistry, 77(1) (2022) 18-25.

64- Pipattanawarothai, A., & Trakulsujaritchok, T. Hybrid polymeric chemosensor bearing rhodamine derivative prepared by sol-gel technique for selective detection of Fe^{3+} ion. Dyes and Pigments, 173(2020) 107946.

65- Heo, J. S., Gil, D., Lee, J. J., & Kim, C. A rhodamine B-based colorimetric chemosensor for sensitive and selective detection of Cu^{2+}: Test strip analysis and density functional theory. Coloration Technology, 139(1) (2023) 4-15.

66- Rha, C. J., Lee, H., & Kim, C. Simultaneous detection of Cu^{2+} and Co^{2+} by a water-soluble carboxamide-based colorimetric chemosensor. ChemistrySelect, 5(3) (2020) 1103-1108.

67- Mohanasundaram, D., Bhaskar, R., Sankarganesh, M., Nehru, K., Kumar, G. G. V., & Rajesh, J. A simple pyridine based fluorescent chemosensor for selective detection of copper ion. Spectrochimica Acta Part A: Molecular and Biomolecular Spectroscopy, 265(2022) 120395.

68- Gigi, G., & Mohan, A. M. Probe-impregnated monolithic polymer as a robust solid-state colorimetric chemosensor for selective sensing of Hg^{2+} in environmental water and cigarette samples. Environmental Research, (2023)115210.

69- Nam, H., Moon, S., Gil, D., & Kim, C. A Dinitrophenol-Based Colorimetric Chemosensor for Sequential Cu^{2+} and S^{2-} Detection. Chemosensors, 11(2) (2023) 143.

70- Haldar, U., Sharma, R., Kim, E. J., & Lee, H. I. Azobenzene–hemicyanine conjugated polymeric chemosensor for the rapid and selective detection of cyanide in pure aqueous media. Journal of Polymer Science, 58(1) (2020) 124-131.

71- Qin, T., Wang, J., Liu, Y., & Guo, S. Carbon Quantum Dots Based Chemosensor Array for Monitoring Multiple Metal Ions. Molecules, 27(12) (2022) 3843.

72- Ooi, C. W., Waldo, U., Norazriena, Y., Lim, K. S., Tan, S. T., Rozalina, Z., & Ahmad, H. L-cysteine grafted fiber-optic chemosensor for heavy metal detection. Optical Fiber Technology, 71(2022) 102938.

73- Mansha, M., Ali, S., Baig, N., & Khan, S. A. Naphthalene-based silica nanoparticles as a highly sensitive fluorescent chemosensor for mercury detection in real seawater. Journal of Molecular Liquids, (2023)121294.

74- Battal, A., Kassa, S. B., Gultekin, N. A., Tavasli, M., & Onganer, Y. A Carbazole-based Fluorescent Turn-off Chemosensor for Iron (II/III) Detection in a Dimethyl Sulfoxide. Journal of Fluorescence, (2023)1-9.